Kybernetika

Rolf Pfiffner; Lino Guzzella
Feedback linearization idle-speed control: design and experiments

Persistent URL: http://dml.cz/dmlcz/135300

FEEDBACK LINEARIZATION IDLE–SPEED CONTROL: DESIGN AND EXPERIMENTS[1]

ROLF PFIFFNER AND LINO GUZZELLA

This paper proposes a novel nonlinear control algorithm for idle-speed control of a gasoline engine. This controller is based on the feedback linearization approach and extends this technique to the special structure and specifications of the idle-speed problem. Special static precompensations and cascaded loops are used to achieve the desired bandwidth separation between the fast spark and slow air-bypass action. A key element is the inclusion of the (engine-speed dependent) induction to power stroke delay in the engine model and in the subsequent controller design. The proposed method is partially validated on an engine test bench using the air paths, only. For the analyzed five cylinder engine, the results show no superior behaviour of the nonlinear approach compared to classical idle-speed controllers. For engines with fewer cylinders, however, the nonlinear approach is expected to perform substantially better.

1. INTRODUCTION

The idle-speed control (ISC) problem is a classical example of an automotive control application. The set-up corresponds to a disturbance rejection problem where the main plant output (engine speed) has to be maintained at a (low) constant value despite the torque disturbances acting on the engine crank-shaft (servo-steering pump, air-conditioning compressor, etc.). The relevance (comfort, fuel consumption, etc.) and the technical challenges (nonlinear plant with large time delays) of this control problem have led to many different control strategies. PID [10], LQ [8], $\mathcal{H}_\infty$ [3, 15], ℓ_1 [2], fuzzy control [1], adaptive control [11], sliding mode [6] and neural networks [13] are some of the frameworks used to treat this problem.

Feedback linearization was investigated in [6] and [9], but the engine's induction to power stroke delay (IPS delay, see [4]) was neglected in these papers. Unfortunately this effect, that depends moreover on the engine speed, is often *the* limiting factor for the controller design. For this reason, the work presented herein approximates this delay with first order low pass elements, which have an engine-speed dependent time constant.

---

[1] Paper presented at the 5th IEEE Mediterannean Conference on Control and Systems held in Paphos (Cyprus) on July 21–23, 1997.

The resulting nonlinear plant with two inputs (air-bypass valve and spark-advance) is not affine in the inputs. However, the plant is shown to be exactly feedback linearizable by introducing additional static compensations. The linearized plant permits the application of well-known linear control design methods. In this paper the different bandwidths of the two input-channels are used in a setting similar to the one presented by [3, 15] to guarantee an optimal engine operation, both under transient and steady-state conditions.

The paper is organized as follows. The notation used is shown in Section 2, and Section 3 introduces the nonlinear engine model in detail. Section 4 treats the feedback linearization of this MIMO model and its application to the idle speed control problem. Due to hardware limitations the experimental verification was possible only for the single-input case, i.e., the ignition channel could not be used for the controller verification. For this reason, in Section 5 the results of Section 4 are specialized to this SISO problem.

Finally, Section 6 shows the results of the experimental verification of the SISO controller. The engine used in the experiments had five cylinders and therefore a rather small IPS delay. Consequently, the proposed nonlinear controller did not behave better than a linear one. However, it is expected that in the case of small cylinder numbers this situation will be different (three or even two cylinder engines are at the moment proposed by many groups for the next generation super efficient "80 miles per gallon" cars).

2. NOTATION

The following notation is used in this paper:

|			
θ :	first input, air-bypass valve	T_l :	engine load torque
$\dot{m}$:	air-bypass valve mass flow rate	T_d :	disturbance torque
P :	intake manifold pressure	K_τ :	delay parameter
P_a :	atmospheric pressure	τ :	IPS delay
T :	intake manifold air temperature	δ :	second input, spark-advance
R :	air gas constant	K_i :	regular load torque parameter
V_m :	intake manifold volume	J_e :	effective engine rotational inertia
$\dot{M}$:	cylinder air mass flow rate	α_i :	model parameter (engine pumping)
N :	engine speed	β_i :	model parameter (throttle-plate)
T_e :	net engine torque	φ_i :	model parameter (engine torque)
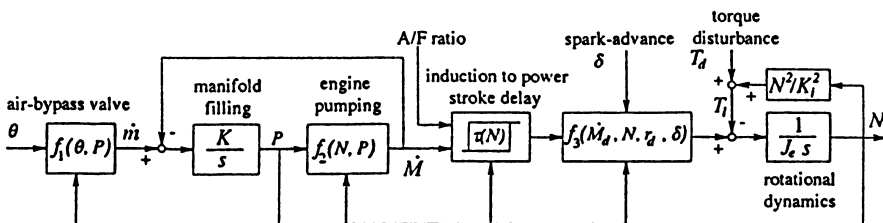
Fig. 1. Nonlinear engine model.

3. NONLINEAR SI–ENGINE MODEL

The nonlinear engine model is based on the work of Powell and Cook [12]. A block diagram of it is presented in Figure 1.

Assumptions. A constant intake manifold temperature, no intake manifold leaks and constant stoichiometric air/fuel-ratio is assumed in this work. Notice that the assumption of neglectable influence of the air/fuel-ratio is acceptable since modern engines are air/fuel-ratio controlled even at idle. At non-idling conditions, where stoichiometric operation is a must to fulfill emission standards, multivariable controls for both speed and air/fuel-ratio are then to be preferred [7].

Under the mentioned assumptions the model of the analyzed plant is described by the following set of equations. For the throttle-plate behaviour

$$\dot{m} = f_1(\theta, P) = f_\theta(\theta) f_P(P) \tag{1}$$

where

$$f_\theta(\theta) = \beta_0 + \beta_1 \theta + \beta_2 \theta^2$$

and

$$f_P(P) = \begin{cases} 1, & P \le P_a/2 \\ \frac{2}{P_a}\sqrt{PP_a - P^2}, & P > P_a/2, \end{cases}$$

for the manifold air-mass-balance

$$\dot{P} = K(\dot{m} - \dot{M}), \text{ where } K = R\,T/V_m, \tag{2}$$

for the engine pumping behaviour

$$\dot{M} = f_2(N, P) = \alpha_0 N P + \alpha_1 N P^2, \tag{3}$$

for the IPS delay

$$\tau = K_\tau/N, \tag{4}$$

for the engine torque output

$$\begin{aligned} T_e &= \varphi_0 + \varphi_1 \dot{M}(t - \tau) + \varphi_2 \delta + \varphi_3 \delta^2 \\ &+ \varphi_4 \delta N + \varphi_5 N + \varphi_6 N^2, \end{aligned} \tag{5}$$

for the load torque

$$T_l = N^2/K_i^2 + T_d \tag{6}$$

and finally, for the engine's rotational dynamic

$$\dot{N} = \frac{1}{J_e}(T_e - T_l). \tag{7}$$

Equations (1)–(7) are the mathematical description of the nonlinear engine model. They are the basis for the following synthesis of the feedback linearization,

the linear feedback controller and for all the MIMO simulations. The numerical values of the model parameters are shown in Appendix A.

The disturbance torque T_d is assumed to be unmeasurable and unpredictable, i.e., all disturbances that are measurable or predictable are assumed to be compensated by a feed-forward controller (not discussed in this paper).

One important aspect of the controller synthesis is the following fact. The control of the engine-speed using the spark-advance path is inherently much faster than using the air-bypass channel. Therefore, a typical ISC transient must be composed of two subsequent periods. In the first part, the controller uses the spark-advance as main input and after that, the engine speed becomes controlled by acting on the air-bypass and the spark-advance returns to its nominal value.

Of course, the first phase should be as short as possible, since during that period a non-ideal combustion takes place (increased fuel consumption, thermal stress, etc.). It is the specific contribution of this paper to investigate approaches that minimize these effects by enhancing the response characteristics of the slower air-channel using nonlinear methods.

4. MULTI–INPUT CASE

4.1. Delay approximation

The IPS delay cannot be described by a finite dimensional ODE. For controller design it is therefore often approximated by rational transfer functions. Moreover, the IPS delay is engine speed dependent. For these reasons it will be approximated below by a first order element whose "time-constant" depends on the inverse engine speed (this corresponds, as will become clearer later, to a bilinear system).

$$\dot{y}(t) = \tilde{\tau}(t)^{-1}(-y(t) + u(t)). \tag{8}$$

This form of the approximation (no finite zeros) is necessary to guarantee that the relative degree of the complete system will be equal to its order and will therefore contain no zero-dynamics [5]. Higher order approximations (several elements (8) in series-connection) are also possible, see Section 5.

The variable $\tilde{\tau}$ is chosen to minimize the error area between the step response $h(t)$ of a linear reference system

$$G(s) = e^{-s\tau(N_0)} \tag{9}$$

and the step-response $\tilde{h}(t)$ of (8) for a fixed engine speed $N = N_0$, i.e.,

$$\int_0^\infty |h(t) - \tilde{h}(t)| \, dt \overset{!}{=} \min. \tag{10}$$

It turns out that the best choice for $\tilde{\tau}$ in the sense of (10) is given by

$$\tilde{\tau} = \frac{\tau(N_0)}{\sigma}, \tag{11}$$

where $\sigma = 1.678346\ldots$.

Remark 1. Notice that the engine speed does not influence the weighting factor σ and that therefore the choice (11) is generally applicable, i.e., that

$$\tilde{\tau}(t) = \frac{\tau(t)}{\sigma} = \frac{K_\tau}{N(t)\,\sigma} \tag{12}$$

is a point-wise optimal solution.

Defining a new state-variable $y = x_2$ and the input $u = \dot{M}$, the description of the IPS delay approximation used below is then given by

$$\dot{x}_2 = \frac{\sigma}{K_\tau} N(\dot{M} - x_2). \tag{13}$$

Remark 2. The proposed approximation works well only if the dynamic of the engine speed N (7) is substantially slower than the dynamic of the cylinder air mass flow rate $\dot{M}$ (3). Fortunately, in typical engine settings this is the case (the manifold pressure P and therefore $\dot{M}$ varies much faster than the engine speed N).

4.2. MIMO feedback linearization

Before discussing the main issue of this section, a slight technical difficulty has to be resolved. The plant description as introduced in (1)–(7) does not fit completely into the usual framework, i.e., the system's equations are not affine in the two inputs. However, by introducing two fictitious new inputs u_1 and u_2 and solving the following two quadratic equations

$$u_1 \;=\; \frac{1}{J_e}\,(\varphi_2 + \varphi_4 N + \varphi_3\,\delta)\,\delta \tag{14}$$

$$u_2 \;=\; \beta_0 + \beta_1\theta + \beta_2\theta^2 \tag{15}$$

(which corresponds to a static nonlinear transformation in each input-channel) the problem can be transformed to its standard form (the ambiguity of the solutions of (14) and (15) can be resolved by physical arguments).

With the above modifications of the system description and the static compensation of the input nonlinearities, the system can be written as follows

$$
\begin{aligned}
\dot{x}_1 &= a_0 + a_1 x_1 + a_2 {x_1}^2 + a_3 x_2 + u_1 - a_d T_d \\
\dot{x}_2 &= a_4 x_1 x_2 + a_5 x_1^2 x_3 + a_6 x_1^2 x_3^2 \\
\dot{x}_3 &= a_7 x_1 x_3 + a_8 x_1 x_3^2 + a_9 f_P(x_3)\, u_2
\end{aligned} \tag{16}
$$

where $x_1 = N$ and $x_3 = P$ and the coefficients a_i follow directly from the "physical" parameters of the model (1)–(7).

The special structure and the time scale separation of the two input channels of this system will play a crucial role in the following considerations. Instead of pursuing a "regular" square MIMO-system feedback linearization [5], a cascade-like

approach is chosen. As a first step the fast spark-channel in (16) is linearized by a precompensation involving the engine speed only

$$u_1 = v_1 - (a_0 + a_1 x_1 + a_2 x_1{}^2) \tag{17}$$

where v_1 is the new spark-channel input. Notice that the link to the (slower) air-channel (represented by the term $a_3 x_2$) is not canceled. Beside the fact that this is not needed (the link is already linear) this would also make little sense for the control problem at hand.

To formalize this step a first coordinate transformation is introduced

$$z_1(t) = x_1(t) \tag{18}$$

and by construction

$$\dot{z}_1 = a_3 x_2 + v_1 - a_d T_d. \tag{19}$$

An obvious choice for a second coordinate transformation is

$$\begin{aligned} z_2(t) &= x_2(t) \\ z_3(t) &= a_4 x_1 x_2 + a_5 x_1^2 x_3 + a_6 x_1^2 x_3^2. \end{aligned} \tag{20}$$

The resulting dynamic equations are

$$\begin{aligned} \dot{z}_2(t) &= z_3 \\ \dot{z}_3(t) &= \varphi(x, v_1) + \psi(x)\, u_2 - \xi(x)\, T_d \end{aligned} \tag{21}$$

where $x = [x_1, x_2, x_3]^T$ and (all time dependencies have been omitted for space reasons)

$$\begin{aligned} \varphi &= (v_1 + a_3 x_2)\,(a_4 x_2 + x_1 x_3\,(2a_5 + 2a_6 x_3)) \\ &\quad + x_1^3 x_3^2\,(a_4 a_6 + a_5 a_8 + 2a_6 a_7 + 2a_6 a_8 x_3) \\ &\quad + a_4^2 x_1^2 x_2 + x_1^3 x_3 a_5\,(a_4 + a_7) \end{aligned} \tag{22}$$

$$\psi = a_9 x_1^2 f_P(x_3)\,(a_5 + 2a_6 x_3)$$

$$\xi = a_d\,\left(a_4 x_2 + 2a_5 x_1 x_3 + 2a_6 x_1 x_3^2\right).$$

Choosing the air bypass control input as follows

$$u_2(t) = \psi(x)^{-1}\,[v_2 - \varphi(x, v_1)] \tag{23}$$

produces an input-output-linearized system whose structure is depicted in Figure 2. The function $\tilde{\xi}(.)$ is defined by

$$\tilde{\xi}(z) = \xi \circ \Phi(z) \tag{24}$$

where $\Phi(z)$ is the inverse coordinate transformation

$$x = \Phi(z) = \begin{bmatrix} z_1 \\ z_2 \\ \frac{-a_5}{2a_6} + \sqrt{\frac{a_5^2}{4a_6^2} - \frac{a_4 z_1 z_2 - z_3}{a_6 z_1^2}} \end{bmatrix} \tag{25}$$

(again, the ambiguity arising from the solution of the involved quadratic equation can be resolved by physical arguments).
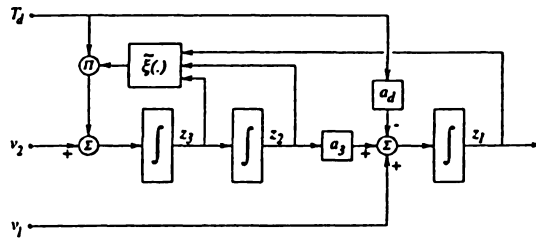

Fig. 2. Structure of the feedback linearized system.

Remark 3. The control (23) is singular for all points on the set defined by $\psi(x) = 0$. However, this set is not relevant for physically meaningful values of the two variables $x_1 = N > 0$ and $x_3 = P > 0$ (the three parameters a_5, a_6 and a_9 are all positive and in idle conditions the manifold pressure P remains always below the ambient pressure P_a).

4.3. MIMO simulations

After having compensated all nonlinearities the next step is to design a linear feedback controller that satisfies all specifications and limitations of the ISC problem. This design-step is performed here for illustration purposes using a cascade-like LQR-approach. The control structure of the complete system with the linear controller is shown in Figure 3.
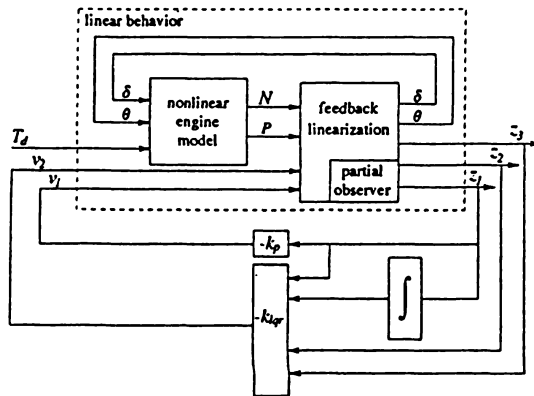

Fig. 3. Control structure of the complete system.

The controls are assumed to have the following bounds

$$\delta \in [-10°, 30°], \quad \theta \in [0°, 90°]. \tag{26}$$

The controller is designed in an hierarchical manner: in a first step the v_1-loop is closed by a proportional feedback k_p, and in a second step the v_2-loop is extended by an additional integrator on the engine speed (to eliminate constant disturbances) and a LQR-regulator k_{lqr} is designed for the remaining SISO plant. The numerical values of the controller parameters used for the simulations are listed in Appendix D. Notice that the controller utilizes 4 states, of which only three (engine speed, integrated engine speed and manifold pressure) are available. The state x_2 has to be estimated using a (partial) observer. The resulting linear controller is of order 2 (one for the partial observer, one for the integral action).

Although the calculated feedback linearization laws (17) and (23) are based on the approximation of the IPS delay, simulations using the exact delay instead of the first order low pass filter, show a very similar behaviour. This fact indicates an inherent robustness of the proposed controller with respect to modelling errors.

The simulations shown in Figure 4 and 5 were performed on the original nonlinear plant, i. e., with the true speed-dependent IPS delay. The achievable responses with the limitations (26) are comparable with those published in previous papers.

The main benefit of the proposed approach is that the different speed requirements for the two input channels can be easily satisfied. In fact the v_1 channel is closely (but not completely) linked to the spark-action. Consequently, manipulating this input substantially influences these dynamics, only. At steady state, with vanishing speed error, the spark-action vanishes, since the spark-controller contains no memory.

The slower air-bypass channel is designed to compensate for constant load torque, i. e., contains one integrator (according to the Internal Model Principle). Its dynamic can be as slow as necessary to satisfy robustness and actuator requirements.
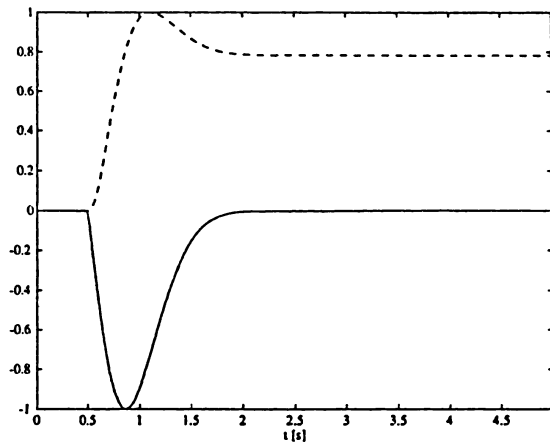

Fig. 4. Normalized state variables: engine speed (solid, nominal value = 740 rpm, range = 60 rpm), manifold pressure (dashed, nominal value = 28 kPa, range = 42 kPa) for a 5 Nm disturbance step.
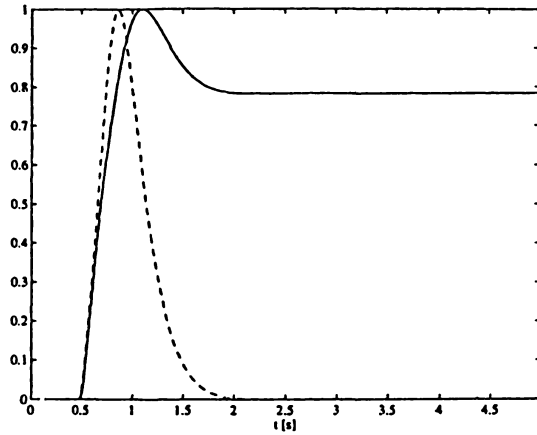
Fig. 5. Normalized control actions: spark (dashed, nominal value $= 15°$, range $= 9°$), air-bypass (solid, nominal value $= 5°$, range $= 6°$) for a 5 Nm disturbance step.

5. SINGLE–INPUT CASE

5.1. Model changes

For the reasons mentioned in Section 1 the spark advance δ is assumed in this section to be constant. Under this assumption, the model of the analyzed plant is described by (1)–(7) with the exception of equation (5) that changes to

$$T_e(t) = \tilde{\varphi}_0 + \tilde{\varphi}_1 \dot{M}(t - \tau(t)) + \tilde{\varphi}_2 N(t) + \tilde{\varphi}_3 N(t)^2. \tag{27}$$

Equations (1)–(7) with the modification (27) are the mathematical description of the nonlinear single-input engine model (the parameters are the same as in the MIMO case, see Appendix A). These equations are the basis for the following synthesis of the feedback linearization, the linear feedback controller and for all the SISO simulations.

Another difference to the MIMO case is introduced by using two (instead of one) elements (8) for the IPS delay approximation (a series connection of any number of elements (8) can be used, with larger numbers producing better approximations but, of course, at higher computational costs; moreover, it can be shown that with increasing number the approximation error tends to zero). The resulting approximation is described by

$$\ddot{q}(t) = \frac{w(t) - [\tilde{\tau}_1(t) + \tilde{\tau}_2(t)]\,\dot{q}(t) - q(t)}{\tilde{\tau}_1(t)\tilde{\tau}_2(t)}. \tag{28}$$

Again, the two variables $\tilde{\tau}_{1,2}(t)$ are chosen to minimize the error area (10) between the step response $h(t)$ of a linear reference system (9) and the step-response $\tilde{h}(t)$ of

(28) for a fixed engine-speed $N = N_0$. It turns out that the best choice for $\tilde{\tau}_{1,2}$ in the sense of (10) is given by

$$\tilde{\tau} = \tilde{\tau}_1 = \tilde{\tau}_2 = \frac{\tau(N_0)}{2.6740\ldots}. \tag{29}$$

Remark 4. Remarks 1 and 2 remain valid in the SISO case, too.

Remark 5. The series connection of two systems (8) in general includes also the derivative of the "time-constant" $\tilde{\tau}(t)$ (and hence the derivative of the the engine-speed)

$$\ddot{q}(t) = \frac{w(t) - 2\tilde{\tau}(t)\dot{q}(t) - q(t)}{\tilde{\tau}(t)^2} - \frac{\dot{\tilde{\tau}}(t)\dot{q}(t)}{\tilde{\tau}(t)}.$$

However, in ISC problems and for typical engine parameters (inertia, engine and load-torque, etc.) the variable $\dot{\tilde{\tau}}(t)$ is much smaller than 2 and can therefore be neglected.

Introducing for (28) the two state-variables x_2 and x_3 with the following dynamics

$$\dot{x}_2(t) \;=\; \frac{1}{\tilde{\tau}(t)}(x_3(t) - x_2(t)) \tag{30}$$

$$\dot{x}_3(t) \;=\; \frac{1}{\tilde{\tau}(t)}(\dot{M}(t) - x_3(t)) \tag{31}$$

the engine-torque (27) can then be approximated by

$$T_e(t) = \tilde{\varphi}_0 + \tilde{\varphi}_1 x_2(t) + \tilde{\varphi}_2 N(t) + \tilde{\varphi}_3 N(t)^2. \tag{32}$$

5.2. SISO feedback linearization

Again, a static precompensation (15) is made first. Defining $x_1 = N$, $x_4 = P$, the system (1)–(7) with (30)–(32) can now be approximated compactly as follows

$$\begin{aligned}
\dot{x}_1 &= a_0 + a_1 x_1 + a_2 x_1^2 + a_3 x_2 - a_d T_d \\
\dot{x}_2 &= a_4 x_1 x_2 + a_5 x_1 x_3 \\
\dot{x}_3 &= a_6 x_1 x_3 + a_7 x_1^2 x_4 + a_8 x_1^2 x_4^2 \\
\dot{x}_4 &= a_9 x_1 x_4 + a_{10} x_1 x_4^2 + a_{11} f_P(x_4)\, u
\end{aligned} \tag{33}$$

where the constants a_i follow in an obvious manner from the original "physical" plant parameters.

With these modifications, the system can be written in the standard input affine form.

$$\begin{aligned}
\dot{x}(t) &= f(x(t)) + g(x(t))\, u(t), \\
y(t) &= h(x(t)) = x_1(t)
\end{aligned} \tag{34}$$

where $x = [x_1, x_2, x_3, x_4]^T$. The specific choice of the engine-speed as output function in equation (34) is somewhat arbitrary (since state-feedback will be applied, any linear combination of the four states is in principle feasible). However, it turns out that this (physically meaningful) choice produces a system (34) with relative degree n and is therefore directly amenable to feedback linearization [5].

In fact, the matrix

$$M(x) = \left[g, ad_f\, g, ad_f^2\, g, ad_f^3\, g \right] (x) \tag{35}$$

(see [5] for the definition of the operator $ad_f^k\, g$) has the determinant

$$\det(M(x)) = a_{11}^4 a_3 a_5^2 x_1^8 \left[a_7 + 2a_8 x_4 \right]^3. \tag{36}$$

All parameters a_i are nonzero, $x_1 = N = 0$ is not possible in this context and the condition $x_4 = P = -a_7/(2a_8)$ is also never satisfied since both a_7 and a_8 are positive. Therefore the matrix $M(x)$ has full rank for all physically meaningful values of the state-variables. This is a sufficient (and also necessary) condition [5] for the existence of a transformation

$$z = \Phi(x) \tag{37}$$

and a feedback

$$u(t) = \frac{a(x(t)) + v(t)}{b(x)} \tag{38}$$

such that in the new coordinates (i.e., from the new input v to the engine-speed) the system after feedback (38) is given by a series connection of four integrators (Brunovsky canonical form) with a nonlinear disturbance injection at each integrator-input

$$\begin{aligned}
\dot{z}_i(t) &= z_{i+1}(t) + \mu_i(z(t))\, T_d(t), \quad i = 1, 2, 3 \\
\dot{z}_4(t) &= v(t) + \mu_4(z(t))\, T_d(t).
\end{aligned} \tag{39}$$

The transformation Φ and the function $a(x)$, defined by

$$\left\langle \frac{\partial z_4}{\partial x}, f \right\rangle (x) \tag{40}$$

($\langle \cdot, \cdot \rangle$ denotes the inner product), are shown in Appendix C. The important fact is that these expressions are polynomial functions of the state-variables only. Therefore, for physically reasonable operating conditions, all expressions remain finite.

Remark 6. The denominator $b(x)$ coincides with the expression (36), which has already been shown to never vanish inside the physically meaningful operating regime. Hence, the proposed control (38) exists for all points x in this region.

5.3. SISO simulations

The validity and the benefits of the proposed approach are first checked by simulations. Three cases have been analyzed:

1) Feedback linearizing controller acting on the nonlinear plant

2) Linear controller acting on the locally linearized plant

3) Linear controller acting on the nonlinear plant.

For each case a "design" and a "simulation" step has to be distinguished. Table 1 summarizes the different cases.
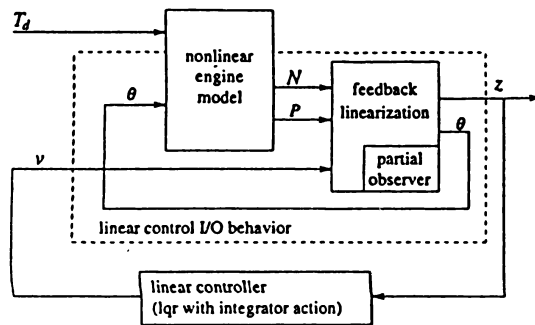

Fig. 6. Control structure of the feedback linearized system.

In case 1) the outer loop (i. e., the loop after compensation (38) of the control-channel nonlinearities of the original plant $(1)-(7)$) is closed with an integral action lqr-controller. This controller is designed to control the linear system (39), i. e., a simple chain of integrators.

Notice that in the plant-model the IPS delay is not approximated by (28) but implemented as a true time delay. The delay approximation (28) introduces two non-physical states, which have to be reconstructed by the "partial observer" within the feedback linearization (see Figure 6).

In case 2) and 3) a controller is used that was synthesized using the linearization of the plant at the nominal engine-speed N_0. For that step the IPS delay is approximated in the same way as in case 1). The design is such that an almost identical closed-loop response is achieved in the linear setting, i. e., in the design phase the engine-speed in case 1) and in case 2) are almost the same.

For the numerical values of the controller parameters see Appendix D.

Table 1. Simulation and design cases.

	design	simulation
case 1)	s^{-4}	nonlinear plant
case 2)	linearized plant	linearized plant
case 3)	linearized plant	nonlinear plant

As Figure 7 shows, the performance of the linear controller degrades quite severely when it acts on the nonlinear plant (case 3), whereas the feedback-linearizing controller (case 1) produces a speed-trajectory that is not affected by the plant's non-linearities.
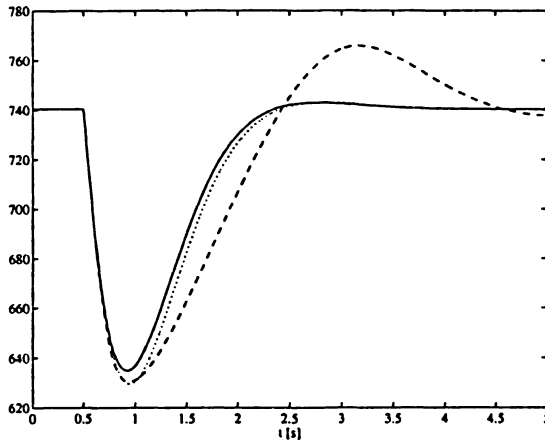

Fig. 7. Engine-speed N (rpm) for case 1) – solid, case 2) – dotted and case 3) – dashed, after a disturbance torque-step of 9 Nm at $t = 0.5$ s.

Of course, there is a price to pay for this superior controller performance. Figure 8 shows that in case 1) the air-bypass has to compensate for the nonlinear effects with substantially larger control action.
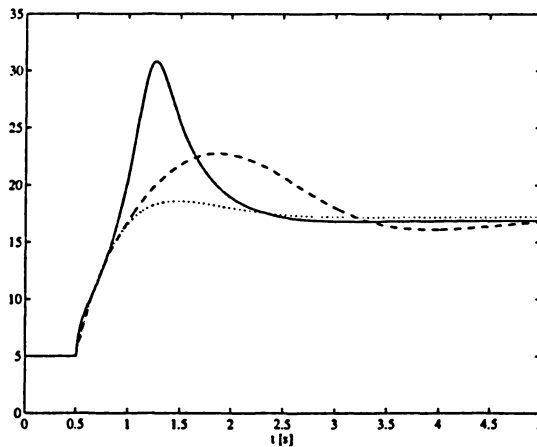

Fig. 8. Air bypass signal θ (degrees) for case 1) – solid, case 2) – dotted and case 3) – dashed, after a disturbance torque-step of 9 Nm at $t = 0.5$ s.

6. EXPERIMENTS

The experimental verification of the proposed SISO controller was done on a 2.2 l five cylinder SI-engine equipped with multi-port fuel injection and (unfortunately) hard-wired ignition system. The engine was mounted on a standard rack and flanged to a dynamometer (see Figure 9). The engine's ISC valve was removed and a very fast bypass valve was installed.
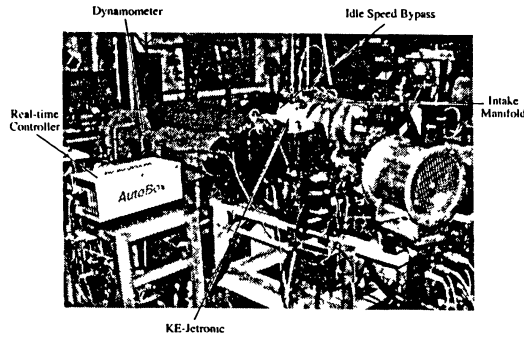

Fig. 9. Test-bench with engine and controller hardware.
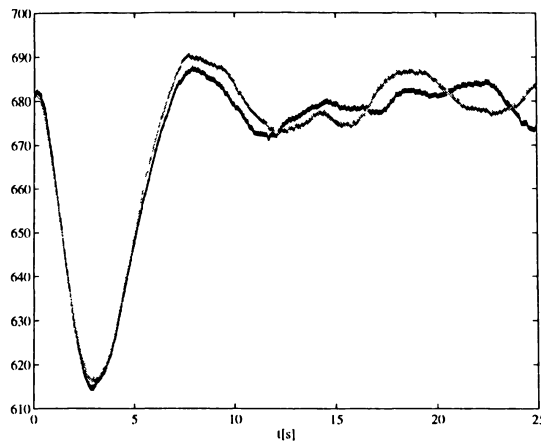
Fig. 10. Measurements of the engine-speed N (rpm) after a disturbance torque-step of 14 Nm at $t = 0.5$ s for case 1) – black and case 3) – gray.

The controller was implemented using commercially available rapid prototyping SW-tools and digital signal processor hardware.

The model parameters used in the simulations were taken from the literature [14]. Therefore, in a first step the corresponding values for the experimental set-up had to be determined. Using static measurements almost all necessary parameters were estimated using (nonlinear) least-squares methods. The "dynamic parameters" K in (2) and J_e in (7) were determined through the comparison of measured step

responses with the corresponding simulations. All values obtained are listed in Appendix B.

Two different controllers (case 1) and case 3) from Section 5) were implemented and tested. The corresponding closed-loop engine-speed responses to a disturbance step of 14 Nm are shown in Figure 10.

No substantial improvements are visible for the nonlinear controller, neither in the measurements nor in the simulations. Obviously, the engine used can be controlled at idle quite well with linear approaches. The system's nonlinearities and its IPS delay variations are not so large that nonlinear controllers would offer substantial advantages (recall, the IPS decreases with increasing number of cylinders).

7. CONCLUSION

In this paper it has been shown that the ISC problem is feedback linearizable even when nonlinear IPS delays are taken into consideration.

Compared with "classical" approaches, nonlinear controllers can enhance the closed-loop performance of ISC, although at the price of higher complexity and larger control action (but not necessarily controller bandwidth!). A detailed analysis of the idle-speed plant and especially of its time delays is crucial.

For the outer linear controller an intuitive design approach, which is based on physical information, remains possible despite the multivariable structure of the plant. The design approach is cascade-like and the physical intuition is not completely lost due to the nonlinear transformations.

The experimental verification of the proposed control algorithm did not show substantial improvements compared to a purely linear approach. This might change when the engine's dynamic is more nonlinear, due for example to smaller cylinder numbers or increased engine nonlinearities.

APPENDIX

A. Engine parameters used for simulations

The engine parameters used for the simulations are taken from [14]. They were adapted to the purpose of this paper.

β_0	=	1	(g/s)	β_1	=	0.907	(g/(s deg))
β_2	=	0.0998	(g/(s deg^2))	α_0	=	0.020	(g/kPa)
α_1	=	$1.054 \cdot 10^{-4}$	(g/(kPa)^2)	K_τ	=	0.75	(-)
φ_0	=	3.922	(N m)	φ_1	=	0.387	(N m s/g)
φ_2	=	$6.350 \cdot 10^{-2}$	(N m/degCA)	φ_3	=	$-1.120 \cdot 10^{-3}$	(N m/(degCA)^2)
φ_4	=	$4.241 \cdot 10^{-4}$	(N m s/degCA)	φ_5	=	$1.357 \cdot 10^{-2}$	(N m s)
φ_6	=	$-4.027 \cdot 10^{-4}$	(N m s^2)	$\bar{\varphi}_0$	=	4.623	(N m)
$\bar{\varphi}_1$	=	0.387	(N m s/g)	$\bar{\varphi}_2$	=	0.020	(N m s)
$\bar{\varphi}_3$	=	$-4.027 \cdot 10^{-4}$	(N m s^2)	P_a	=	101.325	(kPa)
K_i	=	4.386	(1/(m $\sqrt{kg}$))	J_e	=	$0.1760 \cdot (2\pi)$	(m^2 kg)
N_0	=	12.34	(1/s)	T	=	293	(K)
R	=	287	(J/(kg K))	V_m	=	$2.0 \cdot 10^{-3}$	(m^3)

B. Engine parameters of the experiment

The engine parameters of the 2.2 l five cylinder SI-engine were determined using measurements. While these measurements were taken, the engine was operated at stoichiometric air/fuel-ratio. Almost all parameters were estimated using nonlinear least-squares methods applied on static measurements. A different method was applied for the estimation of the "dynamic parameters" K in (2) and J_e in (7). They were determined through the comparison of measured step responses with the corresponding simulations. The following table shows the obtained numerical values of the engine parameters.

β_0	=	3.412	(g/s)	β_1	=	0.0134	(g/(s deg))
β_2	=	$4.323 \cdot 10^{-5}$	(g/(s deg^2))	α_0	=	0.0069	(g/kPa)
α_1	=	$1.251 \cdot 10^{-5}$	(g/(kPa)^2)	K_τ	=	0.6	(-)
$\tilde{\varphi}_0$	=	-2.587	(N m)	$\tilde{\varphi}_1$	=	15.832	(N m s/g)
$\tilde{\varphi}_2$	=	-4.835	(N m s)	$\tilde{\varphi}_3 - 1/(K_i)^2$	=	$-8.695 \cdot 10^{-3}$	(N m s^2)
P_a	=	101.325	(kPa)	J_e	=	$0.2403 \cdot (2\pi)$	(m^2 kg)
N_0	=	11.34	(1/s)	T	=	293	(K)
R	=	287	(J/(kg K))	V_m	=	$4.2 \cdot 10^{-3}$	(m^3)

C. Single–input linearizing control

The following expressions are valid for the case $P \leq P_a/2$ in equation (1) (so called "choked" situation, where the flow through the air by-pass valve reaches sonic conditions in the narrowest part of the orifice). Similar expressions can be derived for the sub-sonic case, but in idle the engine is operated almost all of the time in sonic conditions.

Transformation $z = \Phi(x)$ (37):

$$z_1 = x_1$$

$$z_2 = a_0 + a_1 x_1 + a_2 x_1^2 + a_3 x_2$$

$$z_3 = (a_1 + 2a_2 x_1)(a_0 + a_1 x_1 + a_2 x_1^2 + a_3 x_2) + a_3 x_1 (a_4 x_2 + a_5 x_3)$$

$$z_4 = a_3 x_1 (a_1 + 2a_2 x_1 + a_4 x_1)(a_4 x_2 + a_5 x_3) + a_3 a_5 x_1^2 (a_6 x_3 + a_7 x_1 x_4 + a_8 x_1 x_4^2)$$
$$+ (a_0 + a_1 x_1 + a_2 x_1^2 + a_3 x_2)(a_1^2 + 2a_0 a_2 + 6a_1 a_2 x_1 + 6a_2^2 x_1^2 + 2a_2 a_3 x_2 + a_3 a_4 x_2 + a_3 a_5 x_3)$$

Function $a(x)$ used in (38):

$$a(x) = -a_3 x_1 (a_4 x_2 + a_5 x_3)(a_1^2 + 4a_0 a_2 + a_0 a_4 + 8a_1 a_2 x_1 + 2a_1 a_4 x_1 + 8a_2^2 x_1^2 + 3a_2 a_4 x_1^2 + a_4^2 x_1^2$$
$$+ 4a_2 a_3 x_2 + 2a_3 a_4 x_2 + a_3 a_5 x_3) + a_3 a_5 x_1^4 x_4 (a_9 + a_{10} x_4)(a_7 + 2a_8 x_4)$$
$$+ a_3 a_5 x_1 (a_0 + 2a_1 x_1 + 3a_2 x_1^2 + a_4 x_1^2 + a_6 x_1^2 + a_3 x_2)(a_6 x_3 + a_7 x_1 x_4 + a_8 x_1 x_4^2)$$
$$+ (a_0 + a_1 x_1 + a_2 x_1^2 + a_3 x_2)(a_1^3 + 8a_0 a_1 a_2 + 14 a_1^2 a_2 x_1 + 16 a_0 a_2^2 x_1 + 36 a_1 a_2^2 x_1^2 + 24 a_2^3 x_1^3$$
$$+ 8a_1 a_2 a_3 x_2 + 2a_1 a_3 a_4 x_2 + 16 a_2^2 a_3 x_1 x_2 + 6a_2 a_3 a_4 x_1 x_2 + 2a_3 a_4^2 x_1 x_2 + 2a_1 a_3 a_5 x_3$$
$$+ 6a_2 a_3 a_5 x_1 x_3 + 2a_3 a_4 a_5 x_1 x_3 + 2a_3 a_5 a_6 x_1 x_3 + 3a_3 a_5 a_7 x_1^2 x_4 + 3a_3 a_5 a_8 x_1^2 x_4^2)$$

D. Numerical values of the controller parameters

MIMO state feedback gains   SISO state feedback gains

		case 1)		case 2) & 3)	
$k_{\text{Int}} = 2909.5$	$k_{\text{Int}} = 4.1301 \cdot 10^5$	$k_{\text{Int}} = 10$
$k_{z_1} = 1459.3$	$k_{z_1} = 2.8007 \cdot 10^5$	$k_{x_1} = 4.8403$
$k_{z_2} = 165.06$	$k_{z_2} = 8.1450 \cdot 10^4$	$k_{x_2} = 0.0375$
$k_{z_3} = 21.419$	$k_{z_3} = 5248.7$	$k_{x_3} = 0.0365$
$k_p = 1.3$	$k_{z_4} = 124.07$	$k_{x_4} = 0.0365$

REFERENCES

[1] M. Abate and N. Dosio: Use of Fuzzy Logic for Engine Idle Speed Control. SAE Technical Paper No. 900594, 1990.

[2] K. Butts, N. Sivashankar and J. Sun: Feedforward and feedback design for engine idle speed control using ℓ_1 optimization. In: Proceedings of the American Control Conference, volume 4, 1995, pp. 2587–2590.

[3] C. Carnevale and A. Moschetti: Idle Speed Control With $\mathcal{H}_\infty$ Technique. SAE Technical Paper No. 930770, 1993.

[4] J. A. Cook and B. K. Powell: Modelling of an internal combustion engine for control analysis. IEEE Control Systems Magazine (1988), 20–29.

[5] A. Isidori: Nonlinear Control Systems. Third edition. Springer–Verlag, London Limited 1995.

[6] L. Kjergaard, S. Nielsen, T. Vesterholm and E. Hendricks: Advanced Nonlinear Engine Idle Speed Control Systems. SAE Technical Paper No. 940974, 1994.

[7] Ch. H. Onder and H. P. Geering: Model–based Multivariable Speed and Air–to–fuel Ratio Control of an SI Engine. SAE Technical Paper No. 930859, 1993.

[8] R. L. Morris, M. V. Warlick and R. H. Borcherts: Engine Idle Dynamics and Control: A 5.8l Application. SAE Technical Paper No. 820778, 1982.

[9] S. Nielsen, L. Kjergaard, T. Vesterholm and E. Hendricks: Advanced Nonlinear Engine Idle Speed Control Systems. SAE Technical Paper No. 940974, 1994.

[10] A. W. Olbrot and B. K. Powell: Robust design and analysis of third and fourth order time delay systems with application to automotive idle speed control. In: Proceedings of the American Control Conference, volume 2, 1989, pp. 1029–1039.

[11] M Osawa, H. Ban and M. Miyashita: Stochastic Control for Idle Speed Stability. SAE Technical Paper No. 885066, 1988.

[12] B. K. Powell and J. A. Cook: Nonlinear low frequency phenomenological engine modeling and analysis. In: Proceedings of the American Control Conference, volume 1, 1987, pp. 332–340.

[13] G. V. Puskorius and L. A. Feldkamp: Neurocontrol of nonlinear dynamical systems with Kalman filter trained recurrent networks. IEEE Trans. Neural Networks 5 (1994), 2, 279–297.

[14] F. M. Salam and A. B. Gharbi: Temporal neuro–control of idle engine speed. In: Pro-
     ceedings of the 1996 IEEE International Symposium on Intelligent Control, Dearborn
     1996.
[15] S. J. Williams, D. Hrovat, C. Davey, D. Maclay, J. W. v. Crevel and L. F. Chen: Idle
     speed control design using an $\mathcal{H}_\infty$ approach. In: Proceedings of the American Control
     Conference, volume 3, 1989, pp. 1950–1956.

*Rolf Pfiffner and Lino Guzzella, Engine Systems Laboratory, Swiss Federal Institute of
Technology (ETH), Zürich, CH-8092 Zürich. Switzerland.*
e-mails: r.pfiffner@ieee.org, guzzella@lms.iet.mavt.ethz.ch